Title: Autophagic degradation of the Cucumber mosaic virus virulence factor 2b balances antiviral RNA silencing with proviral plant fitness and virus seed transmission

Short title: Autophagy in CMV disease

Authors;

Aayushi Shukla[¶], Gesa Hoffmann[¶], Silvia López-González, Daniel Hofius and Anders Hafrén*

Affiliations;

Department of Plant Biology, Uppsala BioCenter, Swedish University of Agricultural Sciences and Linnean Center for Plant Biology, Box 7080, 75007 Uppsala, Sweden

*Corresponding author

Email: anders.hafren@slu.se

[¶]These authors contributed equally to this work.

Abstract

Autophagy is a conserved intracellular degradation pathway that has recently emerged as an integral part of plant responses to virus infection. The elucidated mechanisms of autophagy range from the selective degradation of viral components to a more general attenuation of disease symptoms. In addition, several viruses are able to manipulate the autophagy machinery and counteract autophagy-dependent resistance. Despite these findings, the complex interplay of autophagy activities, viral pathogenicity factors, and host defence pathways in disease development remains poorly understood. In the current study, we analysed the interaction between autophagy and Cucumber mosaic virus (CMV) in *Arabidopsis thaliana*. We show that autophagy is induced during CMV infection and promotes the turnover of the major CMV virulence protein and RNA silencing suppressor 2b. Intriguingly, 2b itself dampens plant autophagy. In accordance with 2b degradation, we found that autophagy provides resistance against CMV by reducing viral RNA accumulation in an RNA silencing-dependent manner. Moreover, autophagy and RNA silencing pathways contribute to plant longevity and fecundity of CMV infected plants in an additive manner, uncoupling it from resistance. In addition to reduced fecundity, autophagy-deficient plants also failed to support seed transmission of the virus. We propose that autophagy attenuates CMV virulence via 2b degradation and thereby increases both plant and virus fitness with a trade-off penalty arising from increased RNA silencing-mediated resistance.

Author summary

The capacity of plants to fight pathogenic viruses in order to survive and minimize damage relies on profound cellular reprogramming events. These include the synthesis of new as well as the degradation of pre-existing cellular components, together shifting cellular homeostasis

towards a better tolerance of disease and fortification of antiviral defence mechanisms. Autophagy is a prominent and highly conserved cellular degradation pathway that supports plant stress resilience. Autophagy functions vary broadly and range from rather unspecific renewal of cytoplasm to highly selective degradation of a wide collection of specific substrates. Autophagy is well established to be involved during virus infections in animals, and its importance has also recently emerged in virus diseases of plants. However, we are still far from a comprehensive understanding of the complexity of autophagy activities in host-virus interactions and how autophagy pathway engineering could be applied against viruses. Here, we have analyzed one of the traditional model plant viruses, Cucumber mosaic virus (CMV), and its interactions with autophagy. Our study revealed that autophagy is tightly integrated into CMV disease, influencing processes from plant health to CMV epidemiology.

59 **Introduction**

60 Autophagy is a conserved eukaryotic mechanism that is important for cellular homeostasis
61 through its functions as a major catabolic system. In its simplest form, the autophagy process
62 is considered to sequester cytoplasmic portions non-selectively within a vesicular structure
63 called the autophagosome, which subsequently enters the lytic vacuole of plants for degradation
64 and recycling of nutrients. However, the extent to which autophagy operates in a non-selective
65 manner still remains an open question. In parallel, the examples of selective targeting of
66 autophagic substrates by specialized cargo receptors continues to increase (1, 2). The plant
67 autophagic molecular machinery was initially characterized in *Arabidopsis thaliana* and
68 subsequently recognised in algae, gymnosperms and other angiosperms (3). Core components
69 of this pathway include numerous ATG genes, such as ATG5, ATG7 and ATG8. Selective
70 autophagy is known to take part in the turn-over of substrates including chloroplasts,
71 peroxisomes, aggregates, ribosomes and proteasomes in plants. Selectivity opens the possibility
72 for several highly distinct autophagic processes to operate in parallel, and outlines the important
73 challenge to dissect the overall autophagy effect into its finer mechanisms.

74 Autophagy is induced by numerous environmental conditions, including abiotic stress
75 and nutrient limitation. Its importance for plant adaptation is established in part by the increased
76 sensitivity of autophagy-deficient plants to these conditions (3, 4). Autophagy also plays
77 important roles in plant-pathogen interactions including diseases caused by viruses, bacteria,
78 fungi and oomycetes (5). These studies support the notion that autophagy is a complex process
79 with several functions operating in parallel to influence the infection outcome. Because
80 pathogens commonly cause severe stress to their host plants, it is not surprising that infected
81 plants show an upregulation of autophagy upon infection (6-10). This finding outlines the
82 important concept that the interaction between pathogens and their hosts likely co-evolves in

83 the presence of an activated autophagy response. As a consequence, both pathogen and host
84 could try to utilize the plant autophagy process for their own benefit.

85 In virus-plant interactions, we can distinguish between two mechanisms that limit
86 disease. Host resistance refers to the ability to suppress virus multiplication whereas tolerance
87 is defined as the ability of the plant to minimise the infection-associated damage as a result of
88 the pathogen infection. Co-adaptation of hosts and viruses has resulted in a range of interactions
89 between antiviral resistance mechanisms and viral counter-strategies, together balancing plant
90 and virus fitness (11). Autophagy has been established as a prominent response pathway to
91 several viral infections in the animal field (12). An emerging theme from these studies is that
92 viruses have acquired properties to modify autophagy in many ways, including induction,
93 suppression and subversion of its functions. Evolution of such viral properties can be
94 considered to directly reflect the importance of autophagy for virus infection. Recently,
95 fundamental roles for autophagy have been identified in plant viral diseases, including
96 autophagic degradation of viral components, virus-based counteraction and modulation of
97 autophagy, as well as autophagy-mediated promotion of plant tolerance (7-9, 13, 14).
98 Interestingly, a connection between autophagy and the foremost antiviral defence pathway in
99 plants, RNA silencing, is emerging. Initially, autophagy was suggested to degrade the RNA
100 silencing suppressors of potyviruses (HCpro) and cucumoviruses (2b) (15), and we could
101 recently show that the autophagy cargo receptor NBR1 degrades HCpro to reduce virus
102 susceptibility and accumulation (7). Additionally, autophagy degrades the satellite ßC1 RNA
103 silencing suppressor of geminiviruses, AGO1 when targeted by the poleroviral RNA silencing
104 suppressor P0, and SGS3/RDR6 in the presence of potyviral VPg (9, 16, 17). Notably,
105 autophagy-based resistance was uncoupled from autophagy-based tolerance against a *Potyvirus*
106 (Turnip mosaic virus; TuMV) and a *Caulimovirus* (Cauliflower mosaic virus; CaMV) (7, 8).

107 Thus, autophagy shows complex interactions and a general potential for regulating plant virus
108 disease.

109 In this study we show that autophagy is induced during infection by Cucumber mosaic
110 virus (CMV; genus *Cucumovirus*), a positive-stranded RNA virus. We found that the viral RNA
111 silencing protein 2b has a modest capacity to dampen autophagy and is itself subject to
112 autophagic degradation. Because autophagy suppressed CMV RNA accumulation in an RNA
113 silencing- and AGO1-dependent manner, we propose that 2b degradation represents a
114 resistance mechanism that sensitizes CMV to RNA silencing. In a broader context, autophagy
115 and RNA silencing appear beneficial for CMV infection through synergistic promotion of plant
116 longevity, fecundity and viral seed transmission. Our results thereby reveal that autophagy
117 provides resistance by reducing virus accumulation as well as tolerance by decreasing disease
118 severity during CMV infection, and both processes seem to be linked to the autophagic
119 degradation of the major virulence factor 2b.

120

121 **Results**

122 **Autophagy suppresses disease severity and CMV accumulation**

123 A potential aspect influencing virus and plant fitness is the severity of disease. Previously, we
124 showed that biomass loss, as a measure for disease, was severely increased in loss-of-function
125 mutants of the core autophagy gene ATG5 but not in plants lacking the autophagy cargo
126 receptor NBR1 when infected with TuMV or CaMV (7, 8). In this study, we analysed whether
127 CMV-infected plants showed a similar dependence on functional autophagy by infecting WT,
128 *atg5* and *nbr1* plants with CMV and scoring disease symptoms at 28 days after infection (DAI).
129 While infected WT and *nbr1* plants appeared indistinguishable (Fig 1A) and showed a similar
130 loss in fresh weight (Fig 1B), infected *atg5* plants were severely dwarfed and showed a higher
131 fresh weight loss. We conclude that the core autophagy machinery, but not NBR1 is important

132 for the plant to attenuate CMV disease. This observation is similar to previous findings for
133 TuMV and CaMV (7, 8), and supports a universal role for autophagy in reducing disease
134 symptoms of pathogenic plant viruses.

135 Next, we determined CMV multiplication in WT, *atg5* and *nbr1* plants at 14 DAI (Fig
136 1C). Viral RNA accumulated to higher levels in *atg5* compared to WT and *nbr1* plants. Notably,
137 autophagy-dependent suppression of CMV RNA accumulation was NBR1-independent,
138 distinguishing it from selective autophagy pathways contributing to resistance against CaMV
139 and TuMV (7, 8). We could also detect higher levels of the viral 2b protein in *atg5* compared
140 to WT and *nbr1* plants by Western blotting (Fig 1D), further supporting that autophagy limits
141 CMV accumulation independently of NBR1. We further estimated virus susceptibility by
142 calculating the number of plants showing infection symptoms after mechanical sap inoculation
143 of CMV, and found that infection rate was increased in autophagy-deficient *atg7* mutants
144 compared to WT plants (Fig 1E). Together, these results establish autophagy as a suppressor of
145 CMV infection by decreasing susceptibility, viral RNA accumulation and disease
146 symptomology.

147

148 **Autophagy is induced during CMV infection**

149 Owing to the effect of autophagy in CMV infection (Fig 1), we set out to determine whether
150 autophagy levels were altered during infection. We used an Arabidopsis line that stably
151 expresses GFP-ATG8a, which is a commonly applied marker for detection of autophagosomes.
152 Distribution of this marker was altered in CMV infected tissue, including increased numbers of
153 smaller GFP-ATG8a puncta that likely represented autophagosomes (Fig 2A and B). Infected
154 tissue also contained larger GFP-ATG8a labelled structures that were not observed in healthy
155 tissue. Treatment with concanamycin A (conA), an inhibitor of the vacuolar ATPase, was used
156 to stabilize autophagic bodies delivered into the vacuole (8). The number of GFP-ATGA8a

157 puncta substantially increased upon conA application in infected tissue (Fig 2A and B),
158 suggesting that autophagy is both activated and completed during CMV infection.

159 The processing of free GFP from the GFP-ATG8 fusion protein is regarded as another
160 proxy for autophagy flux in plants. Free GFP levels were higher in CMV infected tissue
161 compared to the healthy control (Fig 2C), supporting elevated autophagy levels. Moreover, we
162 observed higher transcript levels of autophagy-related genes *ATG8a*, *ATG8e* and *NBR1* in CMV
163 infected tissue (Fig 2D), suggesting transcriptional activation of autophagy. NBR1 delivers
164 cargo to autophagosomes and gets degraded in the process, making the NBR1 protein to mRNA
165 ratio another indicator of autophagy activity and flux. Notably, despite elevated *NBR1* transcript
166 levels, there was only slight increase in NBR1 protein accumulation (Fig 2E), suggesting
167 enhanced autophagic degradation during CMV infection. These assays together indicated that
168 autophagy is induced and functional during CMV infection.

169

170 **CMV 2b protein modulates the autophagy response**

171 Our observation of infection-induced autophagy together with the autophagy-dependent
172 suppression of viral RNA accumulation and disease severity prompted us to analyse whether
173 individual CMV proteins could modulate autophagy. First, we used a recently developed
174 quantitative assay in *Nicotiana benthamiana* leaves, that is based on the transient expression of
175 ATG8a fused to *Renilla* luciferase (RLUC) together with firefly luciferase (FLUC) as internal
176 control (6). Co-expression of the viral protein 2b substantially increased RLUC-ATG8a
177 accumulation in relation to FLUC, while 2a, 3a and CP behaved similar as the GUS control
178 (Fig 3A). This result identified 2b as a potential suppressor of autophagy, and as none of the
179 viral proteins seemed to recapitulate infection-induced autophagy on their own, this elevation
180 is likely to be a result of the full infection process. Over-expression of ATG3 was previously
181 shown to induce autophagy in *N. benthamiana* (18) and indeed resulted in a 5-fold increase of

182 FLUC to RLUC-ATG8a ratio (Fig 3B). Additional expression of 2b diminished the inducing
183 effect by ATG3, further supporting the autophagy-suppressing activity of 2b in this system.
184 Importantly, we also found that autophagy was modestly down-regulated in 2b
185 transgenic Arabidopsis seedlings as indicated by a reduced number of GFP-ATG8a labelled
186 autophagosomes in conA treated seedling roots (Fig 3C) and a decreased accumulation of free
187 GFP from GFP-ATG8a (Fig 3D). 2b is the major pathogenicity factor of CMV and 2b
188 transgenic plants show severe growth retardation as well as different morphological
189 abnormalities (19) (Fig 3E). However, the transcript levels for *ATG8a*, *ATG8e* and *NBR1*
190 remained unaffected in 2b transgenic plants (Fig 3F). Thus, the 2b-mediated dampening of
191 autophagy levels appear to occur post-transcriptionally and, 2b pathogenicity alone is not
192 causative for the up-regulation of autophagy pathway transcripts during CMV infection (Fig
193 2D). We therefore conclude that 2b is capable of attenuating the autophagy response.
194
195 **CMV 2b is degraded through autophagy**
196 Previously, autophagy-dependent 2b degradation has been proposed based on its accumulation
197 in response to the PI3K inhibitor 3-methyladenin during transient 2b expression in *N.*
198 *benthamiana* (15). The marked accumulation of the CMV RNA silencing suppressor 2b in *atg5*
199 (Fig 1E) supported this notion that 2b can be degraded by autophagy. Additionally, we also
200 found 2b accumulation in the *atg7* mutant compared to WT (Fig 4A). To further support 2b by
201 autophagy, we performed a GFP-based immunoprecipitation of GFP-ATG8a from mock and
202 CMV infected plants. We found that 2b, but also viral CP, co-purified with GFP-ATG8a (Fig
203 4B), suggesting both proteins may be degraded by autophagy during infection.
204 We further sought to analyse the autophagy-dependent targeting of 2b outside the
205 infection context. We found only a minor stabilization of 2b by conA in transgenic 2b seedlings
206 (Figure 4C), while NBR1 accumulated to substantial amounts, thus verifying the successful

207 inhibitor treatment. We speculated that either the rate of 2b autophagic degradation is slower
208 than that of NBR1 or the stability of these proteins differ in the vacuole. Nonetheless, after
209 introgression of the 2b transgene into the *atg5* background, we found much stronger
210 accumulation of 2b in *atg5* compared to WT (Fig 4D). Notably, NBR1 accumulated to higher
211 levels in WT plants expressing 2b, further supporting 2b-mediated reduction of autophagy. We
212 also noticed that the relative decrease in rosette biomass caused by 2b was much higher in *atg5*
213 plants compared to WT (Fig 4E), which could be a consequence of higher 2b levels, as 2b was
214 shown to facilitate virulence in a concentration-dependent manner (19), and increased
215 sensitivity of *atg5* to 2b virulence.

216 Finally, we carried out co-localization and immunoprecipitation experiments addressing
217 2b and CP association with ATG8a. 2b-RFP, but not CP-RFP, co-localized with GFP-ATG8a
218 in larger cytoplasmic structures (Fig 4F). 2b-RFP was also associated with multiple nuclear
219 speckles including the previously described targeting to the nucleolus (20), and caused re-
220 localization of GFP-ATG8a to the same domains (S1 Fig). CP-RFP also localized to the
221 nucleolus but without recruiting GFP-ATG8a. Interestingly, 2b re-localized CP-GFP but not
222 free GFP to the nuclear sub-compartments during their co-expression (S1 Fig). When 2b-RFP
223 and CP-RFP were co-expressed with either GFP or GFP-ATG8a followed by GFP-based
224 immunoprecipitation, we could detect specific association of 2b with ATG8a. An unspecific
225 signal arising from the RFP-antibody obscured judgement of co-purification of viral CP. Also,
226 no signal was detected in the purified samples using an antibody against CP (not shown), and
227 together with the absence of co-localisation between CP and ATG8a (Figure 4F), CP appears
228 not to be a prominent autophagy target, at least outside of infection. In conclusion, 2b protein
229 associates with ATG8a inside and outside of an infection context.

230

231 **Suppression of CMV RNA accumulation by autophagy involves AGO1 and Dicer proteins**

232 CMV 2b suppresses DCL2- and DCL4-dependent antiviral RNA silencing as shown by restored
233 pathogenicity of 2b-deficient CMV in the *dcl2 dcl4* knock-out mutant (21, 22). Furthermore,
234 2b interacts directly with AGO1 as part of RNA silencing suppression (23). We hypothesized
235 that autophagy could suppress CMV RNA accumulation by compromising 2b-dependent
236 suppression of RNA silencing. If this was the case, autophagy-dependent suppression of CMV
237 RNA accumulation should be less pronounced in *dcl2 dcl4* and *ago1* backgrounds. Indeed,
238 while CMV RNA accumulated to higher levels in both *atg7* and *dcl2 dcl4* mutants, there was
239 no additive effect in the *atg7 dcl2 dcl4* background at 14 DAI (Fig 5A). We obtained similar
240 results for AGO1 as the *ago1 atg5* double mutant did not show any additive increase in CMV
241 RNA accumulation compared to *atg5* and *ago1* single mutants (Fig 5B). The absence of
242 additive effects supports that autophagy and AGO1/DCL2,4-dependent resistance are coupled,
243 likely by autophagy targeting of the viral RNA silencing suppressor 2b.
244
245 **Autophagy and RNA silencing synergistically support plant tolerance to CMV**
246 Despite the apparent non-additive functions of autophagy and RNA silencing in reducing CMV
247 RNA accumulation at early stage of infection (Figure 5A and B), *atg7 dcl2 dcl4* mutants
248 eventually showed a total collapse when infections progressed further (Fig 5C). Notably, there
249 was no tissue senescence in either WT or *dcl2 dcl4* plants, while this autophagy-associated
250 phenotype was clearly visible in CMV-infected *atg7* and highly intensified in *atg7 dcl2 dcl4*
251 plants. When the fresh weight of the rosette was compared as a proxy of disease severity
252 between WT, *atg7*, *dcl2 dcl4* and *atg7 dcl2 dcl4* plants at 28 DAI, a strong additive effect on
253 biomass loss was observed in the combinatorial mutant of autophagy and RNA silencing (Fig
254 5D). We detected a similar dependence on biomass loss between *atg7* and *dcl2 dcl4* for the
255 unrelated dsDNA virus CaMV but not the RNA virus TuMV (S2 Fig). Possibly, TuMV fails to
256 show this dependence owing to very strong suppression of RNA silencing, as biomass loss was

257 overall highest for TuMV and comparable between WT and *dcl2 dcl4* in contrast to CaMV and
258 CMV. The severe biomass loss during CMV infection in the *atg7 dcl2 dcl4* mutants was further
259 corroborated by the loss of chlorophyll (Fig 5E). Because of the severe disease phenotype at 28
260 DAI, we chose to analyse the amount of viral 2b protein per plant as a measure of virus
261 accumulation instead of RT-qPCR. 2b accumulated to clearly higher levels in the single mutants
262 compared to WT (Fig 5F). 2b accumulated to higher levels also in the triple mutant compared
263 to WT when related to the loading control, but whether there are additive effects between *atg7*
264 and *dcl2 dcl4* remained unclear. These results suggested that impaired resistance could
265 contribute to the severe disease phenotype in the *atg7* and *dcl2 dcl4* mutants, and we speculate
266 that the escalated disease phenotype in the triple mutant may be a combination of the failure to
267 undergo partial recovery in *dcl2 dcl4* and enhanced virulence sensitivity in *atg7*.
268
269 **Autophagy is essential for transmission of CMV through seeds**
270 CMV belongs to those plant viruses that also transmit trans-generationally through seeds in a
271 process termed as vertical transmission. Vertical transmission is correlated with plant fecundity,
272 which we found to be substantially more reduced in autophagy-deficient *atg7* compared with
273 WT plants (Fig 6A). Interestingly, CMV infected *dcl2 dcl4* plants failed to produce seeds.
274 Despite reduced fecundity, the seed germination potential remained comparable between *atg7*
275 and WT irrespective of CMV infection (Fig 6B). Finally, we estimated CMV seed transmission
276 in offspring seedlings from infected WT and *atg7* plants. In WT plants, CMV showed a
277 transmission frequency of $1.31 \pm 0.8\%$ when calculated using Gibbs and Gower formulae (Fig
278 6C). This frequency of seed transmission is in the same range that has been reported for other
279 CMV strains in Arabidopsis (24). Notably, we did not detect any seed transmission in *atg7*
280 plants, establishing autophagy as essential for vertical transmission of CMV strain PV0187 in
281 Arabidopsis.

282

283

284 **DISCUSSION**

285 Autophagy can deliver a wide array of substrates including proteins, RNAs, ribosomes,
286 proteasomes, viral particles, organelles and aggregates for degradation in the lytic vacuole (1).
287 Hence, it plays an important role in maintaining plant homeostasis, especially when plants
288 encounter stressful conditions such as viral infections (25). The complexity of substrates
289 targeted by autophagy underscore the possibility that several distinct autophagic processes
290 operate in parallel upon cellular reprogramming and adaption to new conditions. This is
291 fortified by e.g. the uncoupling of autophagy-based plant virus resistance and tolerance against
292 TuMV (7), CaMV (8) and as demonstrated by this study, also CMV. The interaction between
293 CMV and autophagy is complex. It includes resistance and disease attenuation that is coupled
294 to RNA silencing components DCL2/DCL4 and AGO1 as well as autophagy-based degradation
295 of the major virulence factor 2b. Interestingly, 2b alone reduces plant growth in an autophagy-
296 dependent manner and shows a moderate capacity to dampen the autophagy response. The most
297 striking phenotype is the severely increased virulence of CMV during autophagy deficiency
298 that results in reduced plant life span, seed production and vertical virus transmission. Taken
299 together, these multiple connections between autophagy and infection emphasise the
300 complexity of this interaction in CMV epidemiology.

301 Plants reduce pathogen virulence by tolerance and resistance mechanisms, which are
302 assumed to impose different selective pressures on both pathogens and hosts (26). In this study
303 we found that autophagy contributes to the resistance against CMV by reducing virus
304 accumulation. While autophagy-mediated resistance has been established for several animal
305 viruses (12), comparative findings were largely lacking for plant viruses. Only very recently
306 we and others have found that autophagy targets multiple plant viruses, including the positive-

307 stranded RNA viruses TuMV and Barley stripe mosaic virus (7, 14, 27), the negative-stranded
308 RNA virus Rice stripe virus (13), the double-stranded DNA virus CaMV (8) and three single-
309 stranded DNA geminiviruses (9). These findings established autophagy as a central component
310 of plant immunity against viruses, which is fortified further by our current results on CMV.
311 Notably, these studies have revealed a wide mechanistic diversity of autophagy-based virus
312 resistance and viral counter-strategies (25), which ultimately suggests that different plant
313 viruses have co-evolved with the autophagy pathway in an individual manner. However, despite
314 the profound mechanistic differences in the detailed interaction between individual viruses and
315 autophagy, a common theme arising is the involvement of the RNA silencing pathway in the
316 autophagy-virus interplay (25). This connection is evident for CMV as we show that autophagy
317 degrades the viral silencing suppressor 2b and that the enhancement of viral RNA accumulation
318 in autophagy- and RNA silencing-deficient plants lack epistasis. These findings suggest that
319 autophagy-based CMV resistance requires a functional RNA silencing pathway, and we
320 speculate that this is causally linked to the degradation of the viral silencing suppressor 2b.
321 Notably, 2b is a highly complex pathogenicity factor that among other functions interacts with
322 AGO1/4 to impair slicing and also binds siRNAs directly (20, 23, 28, 29). Previously we
323 showed that the TuMV silencing suppressor HCpro is degraded by autophagy, also resulting in
324 reduced virus accumulation (7). Intriguingly, this effect appears to include the degradation of
325 potyvirus-induced structures reminiscent of RNA granules to which also AGO1 localizes (30).
326 Together with the autophagic degradation of the geminiviral satellite ßC1 silencing suppressor
327 (9), autophagy appears to be more generally nested into the antiviral RNA silencing defense
328 with virus-specific adaptations. Opposite to these antiviral roles of autophagy, viral proteins
329 have also been proposed to utilize autophagy for degrading the RNA silencing components
330 SGS3 and AGO1 (16, 17). Taking this into account, we need to consider that autophagy could
331 degrade 2b alone but also in complex with siRNA, AGO1 and other components. At least for

332 HCpro, autophagy seems to target higher-order RNA-protein complexes reminiscent of virus-
333 induced RNA stress granules and processing bodies (7, 30) with likely complex consequences
334 on infection. Whether viral proteins have evolved to function as autophagy cargo receptors to
335 mediate degradation of RNA silencing components is indeed an exciting option. Our results,
336 however, do not support that 2b uses this strategy to counteract RNA silencing-dependent
337 resistance, and in general autophagy seems to support rather than antagonize resistance against
338 plant viruses (7-9, 13, 14, 27).

339 Perhaps the most striking observation in the context of CMV and other viral infections
340 is the escalated disease severity in autophagy-deficient plants (Fig 5). It is likely that elevated
341 2b levels contributes to this phenotype as 2b virulence is dose-dependent (19) and accordingly
342 the growth of 2b transgenic *atg5* is severely reduced compared to 2b transgenic control plants
343 (Fig 4). Defects in RNA silencing alone also increase CMV virulence, but when combined with
344 autophagy deficiency the virulence intensifies to the extent that plants collapse and thus
345 terminate infection. Theory suggests that under strict vertical transmission, virulence should be
346 negatively correlated with the transmission rate (31-33). This can be reasoned because viral
347 fitness is tightly linked to the reproductive success of the host (34). Evidently, optimized
348 virulence benefits virus epidemiology, where virus accumulation and virulence need to be
349 balanced with plant longevity and fecundity to promote both successful horizontal and vertical
350 virus transmission (24, 32, 35). Thus, as autophagy and RNA silencing enhance plant longevity,
351 fecundity and vertical transmission of CMV, the antiviral nature of these pathways in a more
352 holistic and epidemiological context becomes less clear. 2b of CMV subgroup I, including the
353 virulent strains PV0187 (this study) and FNY, but not the mild LS strain of subgroup II,
354 localizes to the nucleolus (20, 36). Interestingly, nucleolar 2b appears to promote virulence
355 uncoupled from virus accumulation and this virulence is furthermore dampened by the RNA
356 silencing pathway (36). This finding is similar to our observation in combined autophagy and

357 RNA silencing knockout mutants. In this context, it is notable that 2b re-localized ATG8a to
358 the nucleolus. Functions associated with nuclear and nucleolar localized LC3, the mammalian
359 homolog of ATG8, are still undefined (37), and so far ATG8 has not been reported in the
360 nucleolus of plants. Despite a potential connectivity between these events, whether 2b-
361 dependent virulence involves nucleolar ATG8 functions remains a matter of future study.

362 2b is a major virulence factor and RNA silencing suppressor of CMV (36) and the strong
363 penalty of super-virulence arising from autophagy- and RNA silencing-deficiency highlights
364 the importance for CMV to fine-tuning these interactions. One exciting possibility is that CMV
365 recruits the autophagy pathway to degrade 2b in a regulated manner to minimize the resistance
366 penalty and support long-term tolerance. At the plant level, virus infections are prolonged
367 processes and the absolute amount of virus can continue to increase for several weeks during
368 systemic infection. However, the active cellular infection cycle is assumed to be largely
369 completed within 24 hours for most plant viruses, including CMV (38). During this relatively
370 short period, CMV may benefit from dampening the autophagy response using 2b without any
371 long-term tolerance costs. It is also interesting that the infection frequency is elevated in
372 autophagy-deficient plants for CMV (Fig 1), TuMV and CaMV (7, 8). This suggests that
373 autophagy suppresses initiation of plant virus infections in general, manifesting the autophagy-
374 virus interaction as most decisive at the very early infection stage. Once the active stage of
375 infection ceases in a cell, the autophagy-mediated clean-up of virulence factors like 2b should
376 promote long-term tolerance and possibly even reduce co-infection competition from weaker
377 viruses that would benefit from high levels of 2b. In line with this, the CP of CMV was recently
378 proposed to destabilize 2b in a self-attenuation mechanism by which the virus achieves long-
379 term virulence reduction (39). At this point, we can only speculate if CP-mediated 2b
380 degradation involves autophagy, but it is interesting that both 2b and CP were present in GFP-
381 ATG8a co-immunoprecipitations from infected plants (Fig 4) and that both proteins localize to

382 the nucleolar virulence domain of 2b (S2 Fig) (36). Nevertheless, our results revealed the
383 autophagic degradation of 2b during transgenic expression in the absence of CP, showing that
384 CP is at least not strictly required in this process. Taken together, we provide a hypothetical
385 model of autophagy as a complex regulator of CMV infection that influences virus
386 accumulation, transmission and plant disease (Fig 7).
387
388
389

390 **Materials and methods**

391 **Plant material and growth conditions**

392 Wild-type (WT) plants were *Arabidopsis thaliana* ecotype Columbia (Col-0). Mutants *atg5-1*,
393 *atg7-2*, *nbr1-2*, *ago1-27*, *dcl2 dcl4, atg7 dcl2 dcl4*, and the GFP-ATG8a transgenic line have
394 been described previously (40-43). The *ago1-27 atg5-1* double mutant was generated by
395 crossing. The transgenic line 2b3C was described previously (19), and used for crossing with
396 GFP-ATG8a and the *atg5-1* background. Arabidopsis plants were grown on soil for infection
397 experiments under short-day conditions (8/16-h light/dark cycles) in a growth cabinet, and
398 *Nicotiana benthamiana* plants were cultivated for transient expression assays under long-day
399 conditions (16/8-h light/dark cycles) in a growth room at 150 µE/m²s, 21°C, and 70% relative
400 humidity, respectively.

401

402 **DNA constructs**

403 *ATG3* and *ATG8a* as well as viral cistrons *2a, 2b, 3a* and *CP* were amplified using cDNA
404 prepared from CMV infected plant total RNA as template and cloned into pENTRY-Topo.
405 *ATG3* was further recombined into pGWB614, and viral proteins into pGWB660 (44).
406 Expression constructs for GUS and GFP-ATG8a were described in (8) and pRD400::*FLUC* in
407 (45). *ATG8a* was recombined into pMDC32:*RLUC* (6) and all binary vectors were transformed
408 into *Agrobacterium* C58C1 for transient expression in *N. benthamiana* or transformation of
409 Arabidopsis by the floral dip method.

410

411 **CMV inoculation and quantification**

412 The first true leaves of 3-week-old Arabidopsis plants were inoculated mechanically with sap
413 prepared from *N. benthamiana* plants infected with the CMV strain PV0187 described in (46).
414 Plants were sampled in biological replicates, each containing 3 individual plants from which

415 inoculated leaves were removed. For CMV RNA or plant transcript quantitation, total RNA
416 was isolated using the RNeasy Plant Mini Kit (Qiagen), and on-column DNA digestion was
417 performed with DNase I (Qiagen). First-strand cDNA was done using Maxima First Strand
418 cDNA Synthesis Kit (Thermo Fisher Scientific). Quantitative RT-PCR analysis (qPCR) was
419 performed with Maxima SYBR Green/Fluorescein qPCR Master Mix (Thermo Fisher
420 Scientific) using the CFX Connect™ Real-Time PCR detection system (BIO-RAD) with gene-
421 specific primers listed in Supplemental Table 1. Normalization was done using *PP2A*
422 (*AT1G69960*).
423

424 **Fresh weight and chlorophyll analysis**

425 Fresh weight refers to the areal rosette of Arabidopsis plants after infection or stable
426 transformation, and is presented as ratios to the respective mock or non-transformed plants. The
427 relative chlorophyll content of plants was determined as described before (8).
428

429 **Confocal microscopy and inhibitor treatment**

430 Live cell images were acquired from abaxial leaf epidermal cells using a Zeiss LSM 780
431 microscope. Excitation/detection parameters for GFP was 488 nm/490-552 nm. Inhibitor
432 treatment was carried out with 0.5 µM concanamycin A in $^{1}/_{2}$ MS 10 h before confocal analysis.
433 Confocal images were processed with ZEN (version 2011). Quantitation of GFP-ATG8a
434 labelled puncta was done using Image J (version 1.48v) software essentially as described in (7).
435

436 **Immunoblot analysis**

437 Proteins were extracted in 100 mM Tris pH 7.5 with 2% SDS, boiled for 5 min in Laemmli
438 sample buffer and cleared by centrifugation. The protein extracts were then separated by SDS-
439 PAGE, transferred to polyvinylidene difluoride (PVDF) membranes (Amersham, GE

440 Healthcare), blocked with 5% skimmed milk in PBS, and incubated with primary antibodies
441 anti-NBR1 (47), anti-2b (20), anti-CP (Bioreba Art.Nr. 160612), anti-GFP (Santa Cruz
442 Biotechnology; sc-9996) using 1:2000 dilution in PBS 0.1% Tween-20, and secondary
443 horseradish peroxidase-conjugated antibodies 1:10 000 in PBS 0.1% Tween-20 (Amersham,
444 GE Healthcare). The immunoreaction was developed using the ECL Prime kit (Amersham, GE
445 Healthcare) and detected in a LAS-3000 Luminescent Image Analyzer (Fujifilm, Fuji Photo
446 Film).
447
448 **Immunoprecipitation**
449 For immunoprecipitation, plant tissue was homogenized in 2 ml buffer (100 mM Tris pH8, 150
450 mM NaCl, 0.5% TX-100, protease inhibitor cocktail (Roche)) per gram of tissue. The lysate
451 was cleared at 4000 x g for 5 min at 4°C, filtered through two layers of miracloth and incubated
452 1h with anti-GFP µbeads according to manufacturer's instruction (Milteney) for infected
453 Arabidopsis tissue and GFP-agarose beads (Chromotech) for transiently expressing *N.*
454 *benthamiana* tissue. After washing 4 times with buffer, samples were eluted using 2x Laemmli
455 sample buffer and analyzed by immunoblotting.
456
457 **Analysis of fecundity, germination potential and vertical virus transmission**
458 Plants grown under long-day conditions were infected with CMV and allowed to set seeds. The
459 seed weight was recorded and the relative fecundity is presented as a ratio between seeds from
460 control and infected plants. Seed germination potential of offspring seeds was recorded after
461 calculating the percentage of germinated seeds on ½ MS plates supplemented with 1% sucrose.
462 For vertical transmission, 10 pools of 20 seedlings each were analysed by RT-PCR per parental
463 plant for presence of CMV. Probability of virus transmission by a single seed was calculated
464 by the Gibbs and Gower's formulae (48) $p = 1 - \left(1 - \frac{y}{n}\right)^{1/k}$; where p is the probability of

465 virus transmission by a single seed, y is the number of positive samples, n denotes the total
466 number of samples assayed and k represents the number of seedlings taken per sample.
467
468 **Data analysis and presentation**
469 Data are presented as mean ± standard deviation (SD) and statistical significance was analyzed
470 by two-sided Student´s *t*-test with *p*-values <0.05 denoted * and *p*-values <0.01 denoted **.
471 The number of replicates is given in the respective figure legends (*n*).
472
473
474 **Acknowledgements**
475 We gratefully acknowledge John Carr for providing the CMV PV0187 strain and 2b transgenic
476 lines as well as Thomas Canto for the 2b antibody.
477
478
479 **Reference**
480 1. Batoko H, Dagdas Y, Baluska F, Sirko A. Understanding and exploiting autophagy
481 signaling in plants. Essays in biochemistry. 2017;61(6):675-85.
482 2. Rogov V, Dotsch V, Johansen T, Kirkin V. Interactions between autophagy receptors
483 and ubiquitin-like proteins form the molecular basis for selective autophagy. Mol Cell.
484 2014;53(2):167-78.
485 3. Michaeli S, Galili G, Genschik P, Fernie AR, Avin-Wittenberg T. Autophagy in Plants--
486 What's New on the Menu? Trends Plant Sci. 2016;21(2):134-44.
487 4. Soto-Burgos J, Zhuang X, Jiang L, Bassham DC. Dynamics of Autophagosome
488 Formation. Plant physiology. 2018;176(1):219-29.

489 5. Hofius D, Li L, Hafren A, Coll NS. Autophagy as an emerging arena for plant-pathogen
490 interactions. Current opinion in plant biology. 2017;38:117-23.
491 6. Ustun S, Hafren A, Liu Q, Marshall RS, Minina EA, Bozhkov PV, et al. Bacteria Exploit
492 Autophagy for Proteasome Degradation and Enhanced Virulence in Plants. The Plant cell.
493 2018;30(3):668-85.
494 7. Hafren A, Ustun S, Hochmuth A, Svenning S, Johansen T, Hofius D. Turnip Mosaic Virus
495 Counteracts Selective Autophagy of the Viral Silencing Suppressor HCpro. Plant physiology.
496 2018;176(1):649-62.
497 8. Hafren A, Macia JL, Love AJ, Milner JJ, Drucker M, Hofius D. Selective autophagy limits
498 cauliflower mosaic virus infection by NBR1-mediated targeting of viral capsid protein and
499 particles. Proceedings of the National Academy of Sciences of the United States of America.
500 2017;114(10):E2026-E35.
501 9. Haxim Y, Ismayil A, Jia Q, Wang Y, Zheng X, Chen T, et al. Autophagy functions as an
502 antiviral mechanism against geminiviruses in plants. Elife. 2017;6.
503 10. Dagdas YF, Belhaj K, Maqbool A, Chaparro-Garcia A, Pandey P, Petre B, et al. An
504 effector of the Irish potato famine pathogen antagonizes a host autophagy cargo receptor.
505 Elife. 2016;5.
506 11. Paudel DB, Sanfacon H. Exploring the Diversity of Mechanisms Associated With Plant
507 Tolerance to Virus Infection. Front Plant Sci. 2018;9:1575.
508 12. Dong XN, Levine B. Autophagy and Viruses: Adversaries or Allies? J Innate Immun.
509 2013;5(5):480-93.
510 13. Fu S, Xu Y, Li C, Li Y, Wu J, Zhou X. Rice Stripe Virus Interferes with S-acylation of
511 Remorin and Induces Its Autophagic Degradation to Facilitate Virus Infection. Mol Plant.
512 2018;11(2):269-87.

513 14. Yang M, Zhang Y, Xie X, Yue N, Li J, Wang XB, et al. Barley stripe mosaic virus gammab
514 Protein Subverts Autophagy to Promote Viral Infection by Disrupting the ATG7-ATG8
515 Interaction. The Plant cell. 2018;30(7):1582-95.
516 15. Nakahara KS, Masuta C, Yamada S, Shimura H, Kashihara Y, Wada TS, et al. Tobacco
517 calmodulin-like protein provides secondary defense by binding to and directing degradation
518 of virus RNA silencing suppressors. Proceedings of the National Academy of Sciences of the
519 United States of America. 2012;109(25):10113-8.
520 16. Cheng X, Wang A. The Potyvirus Silencing Suppressor Protein VPg Mediates
521 Degradation of SGS3 via Ubiquitination and Autophagy Pathways. Journal of virology.
522 2017;91(1).
523 17. Derrien B, Baumberger N, Schepetilnikov M, Viotti C, De Cillia J, Ziegler-Graff V, et al.
524 Degradation of the antiviral component ARGONAUTE1 by the autophagy pathway.
525 Proceedings of the National Academy of Sciences of the United States of America.
526 2012;109(39):15942-6.
527 18. Han S, Wang Y, Zheng X, Jia Q, Zhao J, Bai F, et al. Cytoplastic Glyceraldehyde-3-
528 Phosphate Dehydrogenases Interact with ATG3 to Negatively Regulate Autophagy and
529 Immunity in Nicotiana benthamiana. The Plant cell. 2015;27(4):1316-31.
530 19. Lewsey M, Robertson FC, Canto T, Palukaitis P, Carr JP. Selective targeting of miRNA-
531 regulated plant development by a viral counter-silencing protein. The Plant journal : for cell
532 and molecular biology. 2007;50(2):240-52.
533 20. Gonzalez I, Martinez L, Rakitina DV, Lewsey MG, Atencio FA, Llave C, et al. Cucumber
534 mosaic virus 2b protein subcellular targets and interactions: their significance to RNA silencing
535 suppressor activity. Molecular plant-microbe interactions : MPMI. 2010;23(3):294-303.

536 21. Diaz-Pendon JA, Li F, Li WX, Ding SW. Suppression of antiviral silencing by cucumber
537 mosaic virus 2b protein in Arabidopsis is associated with drastically reduced accumulation of
538 three classes of viral small interfering RNAs. The Plant cell. 2007;19(6):2053-63.
539 22. Ziebell H, Carr JP. Effects of dicer-like endoribonucleases 2 and 4 on infection of
540 Arabidopsis thaliana by cucumber mosaic virus and a mutant virus lacking the 2b counter-
541 defence protein gene. The Journal of general virology. 2009;90(Pt 9):2288-92.
542 23. Zhang X, Yuan YR, Pei Y, Lin SS, Tuschl T, Patel DJ, et al. Cucumber mosaic virus-encoded
543 2b suppressor inhibits Arabidopsis Argonaute1 cleavage activity to counter plant defense.
544 Genes & development. 2006;20(23):3255-68.
545 24. Pagan I, Fraile A, Fernandez-Fueyo E, Montes N, Alonso-Blanco C, Garcia-Arenal F.
546 Arabidopsis thaliana as a model for the study of plant-virus co-evolution. Philos Trans R Soc
547 Lond B Biol Sci. 2010;365(1548):1983-95.
548 25. Kushwaha NK, Hafren A, Hofius D. Autophagy-virus interplay in plants: from antiviral
549 recognition to proviral manipulation. Mol Plant Pathol. 2019;20(9):1211-6.
550 26. Roy BA, Kirchner JW. Evolutionary dynamics of pathogen resistance and tolerance.
551 Evolution. 2000;54(1):51-63.
552 27. Li F, Zhang C, Li Y, Wu G, Hou X, Zhou X, et al. Beclin1 restricts RNA virus infection in
553 plants through suppression and degradation of the viral polymerase. Nat Commun.
554 2018;9(1):1268.
555 28. Zhao JH, Liu XL, Fang YY, Fang RX, Guo HS. CMV2b-Dependent Regulation of Host
556 Defense Pathways in the Context of Viral Infection. Viruses. 2018;10(11).
557 29. Goto K, Kobori T, Kosaka Y, Natsuaki T, Masuta C. Characterization of silencing
558 suppressor 2b of cucumber mosaic virus based on examination of its small RNA-binding
559 abilities. Plant Cell Physiol. 2007;48(7):1050-60.

560 30. Hafren A, Lohmus A, Makinen K. Formation of Potato Virus A-Induced RNA Granules
561 and Viral Translation Are Interrelated Processes Required for Optimal Virus Accumulation.
562 PLoS pathogens. 2015;11(12):e1005314.
563 31. Elena SF, Agudelo-Romero P, Carrasco P, Codoner FM, Martin S, Torres-Barcelo C, et
564 al. Experimental evolution of plant RNA viruses. Heredity (Edinb). 2008;100(5):478-83.
565 32. Lenski RE, May RM. The evolution of virulence in parasites and pathogens:
566 reconciliation between two competing hypotheses. J Theor Biol. 1994;169(3):253-65.
567 33. Alizon S, Hurford A, Mideo N, Van Baalen M. Virulence evolution and the trade-off
568 hypothesis: history, current state of affairs and the future. J Evol Biol. 2009;22(2):245-59.
569 34. Lipsitch M, Siller S, Nowak MA. The Evolution of Virulence in Pathogens with Vertical
570 and Horizontal Transmission. Evolution. 1996;50(5):1729-41.
571 35. Stewart AD, Logsdon JM, Jr., Kelley SE. An empirical study of the evolution of virulence
572 under both horizontal and vertical transmission. Evolution. 2005;59(4):730-9.
573 36. Du Z, Chen A, Chen W, Liao Q, Zhang H, Bao Y, et al. Nuclear-cytoplasmic partitioning
574 of cucumber mosaic virus protein 2b determines the balance between its roles as a virulence
575 determinant and an RNA-silencing suppressor. Journal of virology. 2014;88(10):5228-41.
576 37. Kraft LJ, Manral P, Dowler J, Kenworthy AK. Nuclear LC3 Associates with Slowly
577 Diffusing Complexes that Survey the Nucleolus. Traffic. 2016;17(4):369-99.
578 38. Gonda T, Symons R. Cucumber Mosaic Virus Replication in Cowpea Protoplasts: Time
579 Course of Virus, Coat Protein and RNA Synthesis. Journal of General Virology. 1979;45:723-
580 736.
581 39. Zhang XP, Liu DS, Yan T, Fang XD, Dong K, Xu J, et al. Cucumber mosaic virus coat
582 protein modulates the accumulation of 2b protein and antiviral silencing that causes symptom
583 recovery in planta. PLoS pathogens. 2017;13(7):e1006522.

584 40. Hofius D, Schultz-Larsen T, Joensen J, Tsitsigiannis DI, Petersen NH, Mattsson O, et al.
585 Autophagic components contribute to hypersensitive cell death in Arabidopsis. Cell.
586 2009;137(4):773-83.
587 41. Yoshimoto K, Jikumaru Y, Kamiya Y, Kusano M, Consonni C, Panstruga R, et al.
588 Autophagy negatively regulates cell death by controlling NPR1-dependent salicylic acid
589 signaling during senescence and the innate immune response in Arabidopsis. The Plant cell.
590 2009;21(9):2914-27.
591 42. Zhou J, Wang J, Cheng Y, Chi YJ, Fan B, Yu JQ, et al. NBR1-mediated selective autophagy
592 targets insoluble ubiquitinated protein aggregates in plant stress responses. PLoS genetics.
593 2013;9(1):e1003196.
594 43. Munch D, Teh OK, Malinovsky FG, Liu Q, Vetukuri RR, El Kasmi F, et al. Retromer
595 contributes to immunity-associated cell death in Arabidopsis. The Plant cell. 2015;27(2):463-
596 79.
597 44. Nakagawa T, Kurose T, Hino T, Tanaka K, Kawamukai M, Niwa Y, et al. Development of
598 series of gateway binary vectors, pGWBs, for realizing efficient construction of fusion genes
599 for plant transformation. Journal of bioscience and bioengineering. 2007;104(1):34-41.
600 45. Eskelin K, Suntio T, Hyvarinen S, Hafren A, Makinen K. Renilla luciferase-based
601 quantitation of Potato virus A infection initiated with Agrobacterium infiltration of N.
602 benthamiana leaves. J Virol Methods. 2010;164(1-2):101-10.
603 46. Groen SC, Jiang S, Murphy AM, Cunniffe NJ, Westwood JH, Davey MP, et al. Virus
604 Infection of Plants Alters Pollinator Preference: A Payback for Susceptible Hosts? PLoS
605 pathogens. 2016;12(8):e1005790.

606 47. Svenning S, Lamark T, Krause K, Johansen T. Plant NBR1 is a selective autophagy
607 substrate and a functional hybrid of the mammalian autophagic adapters NBR1 and
608 p62/SQSTM1. Autophagy. 2011;7(9):993-1010.
609 48. Gibbs, A. J.; Gower, J. C. 1960: The use of a multiple transfer method in plant virus
610 transmission studies—some statistical points arising from the analysis of resuhs. Annals of
611 Applied Biology 48: 75-83.
612
613

614 **Figures**

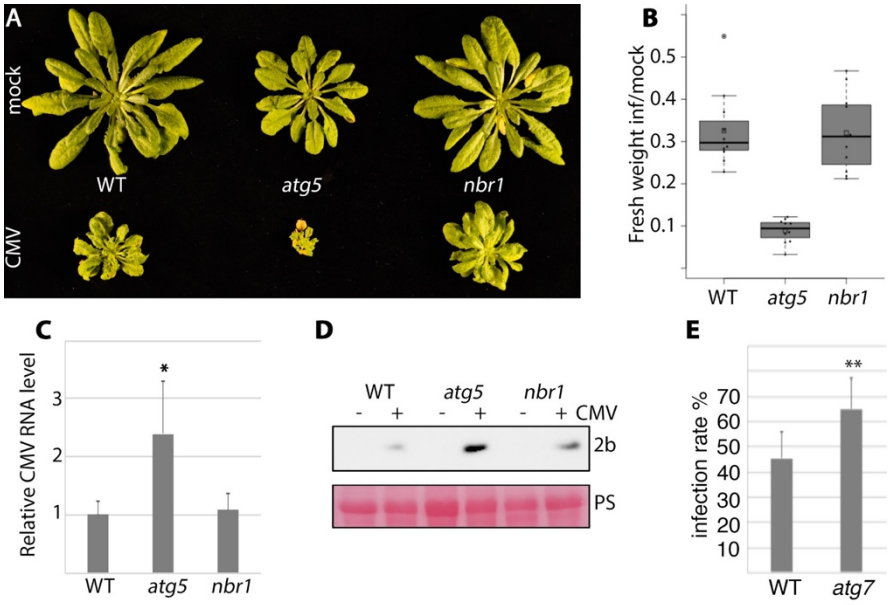

615

616

617 **Fig 1. Autophagy promotes plant tolerance and resistance against CMV infection**

618 A) Representative WT (Col-0), *atg5* and *nbr1* plants at 28 days after mock or CMV inoculation.
619 B) The fresh weight ratio of CMV infected to mock plants 28 days after inoculation (DAI).
620 (n=9). C) Relative CMV RNA levels determined by RT-qPCR at 14 DAI. (n=4). D) In parallel
621 with (C), protein samples were prepared and CMV protein 2b was detected by Western blotting
622 using anti-2b. NBR1 detection was used to verify *atg5* and *nbr1* mutants and Rubisco large
623 subunit was visualized by Ponceau S staining (PS) of the membrane as loading control. E) CMV
624 infection rate in WT and *atg7* plants determined by presence/absence of viral symptoms three
625 weeks after mechanical sap inoculation. (n=8). Statistical significance (*P<0.05; **P<0.01)
626 was revealed by Student´s t-test (compared to WT).

627

628

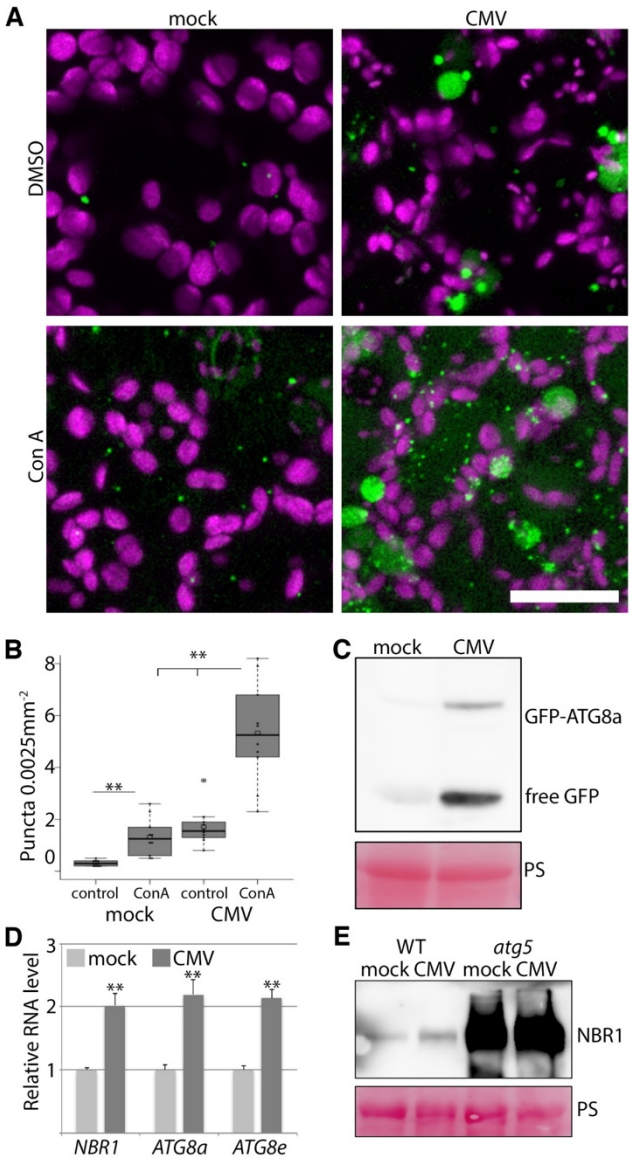

629

630

631 **Fig 2. Autophagy is activated and functional during CMV infection**

632 A) Representative images of the GFP-ATG8a marker in healthy and CMV infected plants

633 with and without concanamycin A (conA) treatment. Chloroplasts are shown in magenta.

634 Images are confocal Z-stacks. Scale bar = 20 µm. B) GFP-ATG8a foci were counted from

635 similar images as in (A) using Image J. (*n*=10). C) Western blot analysis of free GFP levels

636 derived from GFP-ATG8a in mock and CMV infected plants. Ponceau S (PS) staining

637 verified comparable protein loading. D) Transcript levels for *NBR1*, *ATG8a* and *ATG8e* in

638 mock and CMV infected plants were determined by RT-qPCR. (*n*=4). E) Western blot

639 detection of NBR1 levels in mock and CMV inoculated WT and *atg5* plants. Ponceau S (PS)

640 staining verified comparable protein loading. Statistical significance (*P<0.05; **P<0.01)

641 was revealed by Student´s *t*-test (compared to WT).

642

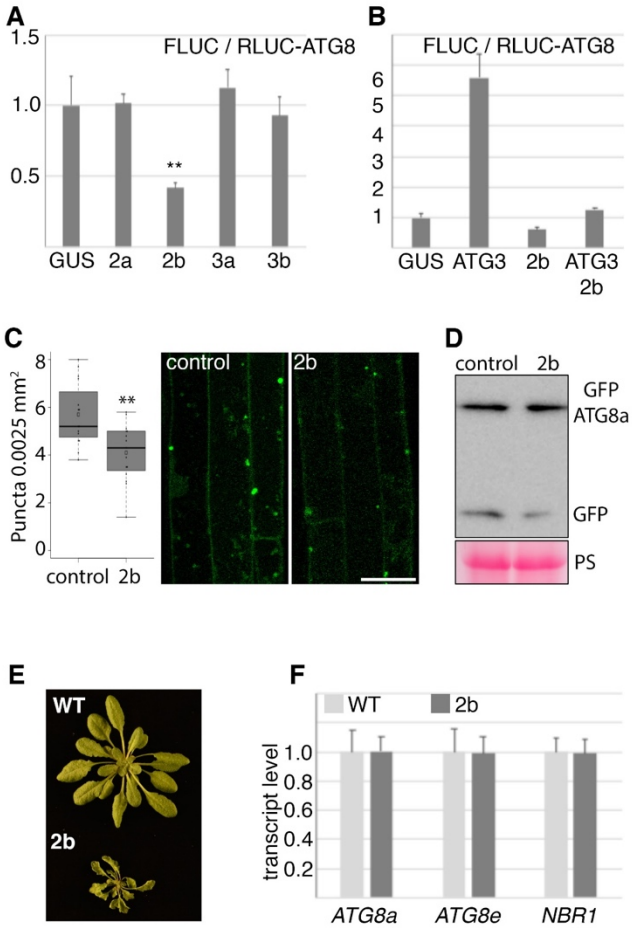

643

644 **Fig 3. CMV protein 2b can dampen autophagy**

645 A) RLUC-ATG8a and the internal control FLUC were co-expressed with viral proteins and
646 GUS in leaves of *N. benthamiana*. Normalized luciferase values are given as a ratio between
647 FLUC and RLUC, resulting in decreased ratios when RLUC-ATG8a degradation is reduced.
648 (*n*=4). B) As in (A), but co-expressed proteins where GUS, ATG3, 2b and ATG3+2b. (*n*=4).
649 C) The number of GFP-ATG8a foci were analyzed in roots of 10-day old seedlings without and
650 with stable expression of 2b after 10h conA treatment. Counting was performed using ImageJ
651 particle analyzer on confocal Z-stack projections. (*n*=15). Representative images are shown
652 with scale bar = 20 µm. D) Anti-GFP western blot analysis was performed in parallel with (C)
653 to estimate the ratio of GFP-ATG8a to free GFP. Rubisco large subunit visualized by Ponceau
654 S staining (PS) of the membrane is shown as loading control. E) Representative image of 4-
655 week-old short-day grown 2b expression line in comparison to WT plants. H) Transcript levels

656 of *ATG8a*, *ATG8e* and *NBR1* were determined by RT-qPCR using *PP2a* as reference from

657 plants shown in (E). (n=4). Statistical significance (**P<0.01) was revealed by Student´s t-test.

658

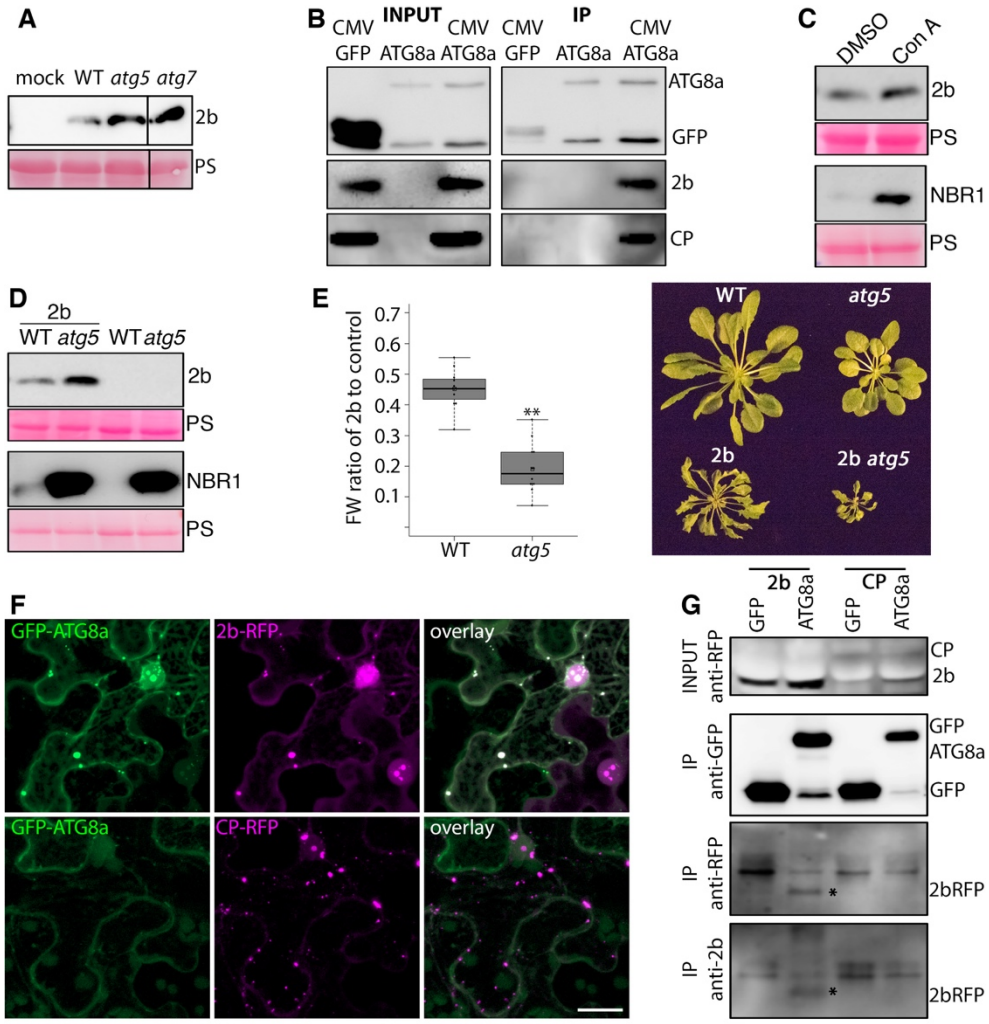

Fig 4. Autophagy degrades CMV 2b both in and outside the infection context

A) Accumulation of viral 2b protein was determined in WT, *atg5* and *atg7* plants at 14 DAI by western blot analysis. B) Co-immunoprecipitation analysis of viral CP and 2b with GFP-ATG8a from infected transgenic Arabidopsis tissue. Non-infected GFP-ATG8a and infected GFP expressing plants were used as control. Shown are the input and immunoprecipitated (IP) samples. C) 2b transgenic seedlings were treated with DMSO (control) or concanamycin A for 10h followed by western blot detection of 2b. Increased accumulation of NBR1 verified the concanamycin A (conA) treatment. D) Accumulation of 2b in transgenic WT and *atg5* plants was analyzed by western blotting. Increased accumulation of NBR1 verified the *atg5* background. Ponceau S-stained Rubisco shows loading (PS) in (A, C and D). E) 2b-dependent

671 virulence measured as relative fresh weight loss caused by transgenic 2b expression compared
672 to non-transgenic plants in WT and *atg5* backgrounds. (*n*=9). A representative plant image is
673 shown to the right. F) Co-localization analysis in *N. benthamiana* leaves co-expressing 2b-RFP
674 or CP-RFP with GFP-ATG8a. These Z-stack images were acquired 48 h post agroinfiltration.
675 Scale bar = 20 μm. G) Co-precipitation analysis of 2b-RFP and CP-RFP with GFP-ATG8a in
676 parallel with (F). Expression of GFP was used as control. Shown is the anti-RFP input signal,
677 as well as anti-GFP, anti-RFP and anti-2b signals from the GFP-based immunoprecipitated
678 samples. The position of 2b-RFP is marked with an asterisk.
679
680
681
682
683

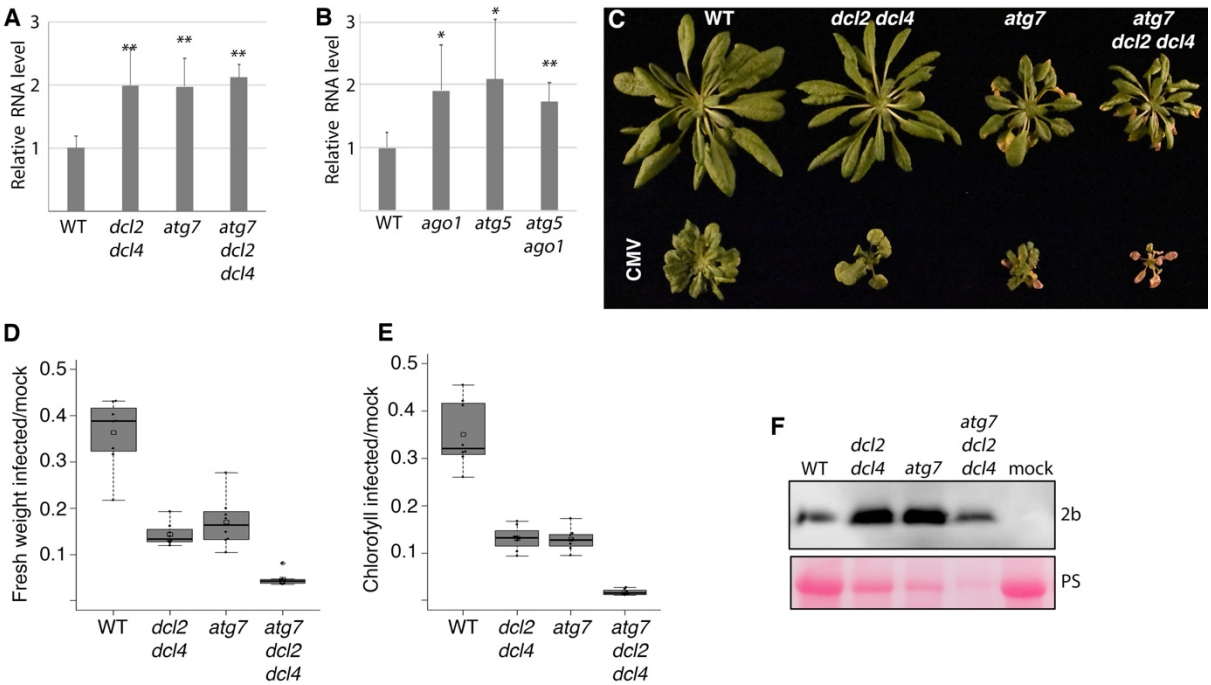

Fig 5. Autophagy-enhanced CMV resistance and tolerance are uncoupled and involve RNA silencing.

A) Relative CMV RNA levels determined by RT-qPCR at 14 DAI in WT, *atg7*, *dcl2 dcl4* and *atg7 dcl2 dcl4* plants (*n*=4). B) Relative CMV RNA levels determined by RT-qPCR at 14 DAI in WT, *atg5*, *ago1* and *atg5 ago1* plants (*n*=4). C) Representative image of mock-and CMV inoculated plants at 28 DAI. D and E) Relative fresh weight (D) and chlorophyll content (E) in CMV infected plants compared to mock at 28 DAI. (*n*=10). F) Western blot analysis of CMV 2b protein accumulation per plant in parallel with (C, D, E). Ponceau S stained Rubisco shows loading (PS) and reveals reduced total protein content per plant in the mutants compared WT.

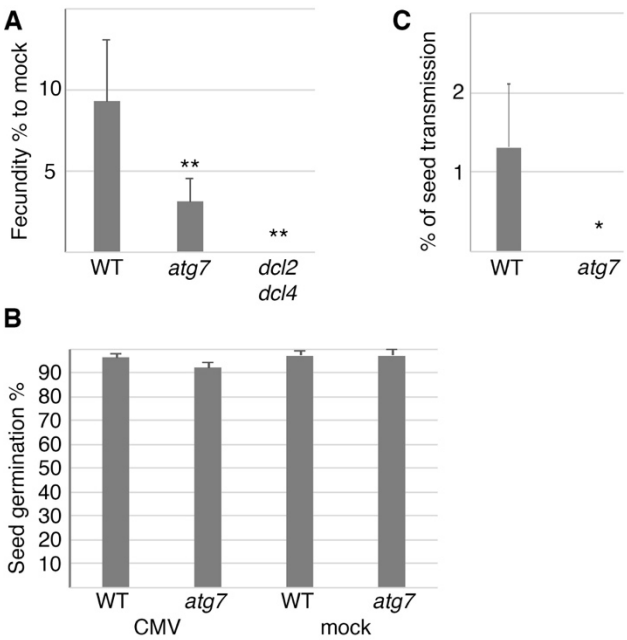

698

699 **Fig 6. Autophagy and RNA silencing is essential for vertical transmission of CMV**

700 A) Total seed weight of infected WT, *atg7* and *dcl2 dcl4* plants presented as a percentage

701 relative to seeds produced by non-infected mock plants. (*n*=5). B) The percentage of seeds

702 germinating from infected and non-infected WT and *atg7* plants. (*n*=5). C) Vertical

703 transmission of CMV was estimated by RT-PCR in seedlings derived from seeds of infected

704 WT and *atg7* plants (*n*=5 independent plants).

705

706

707

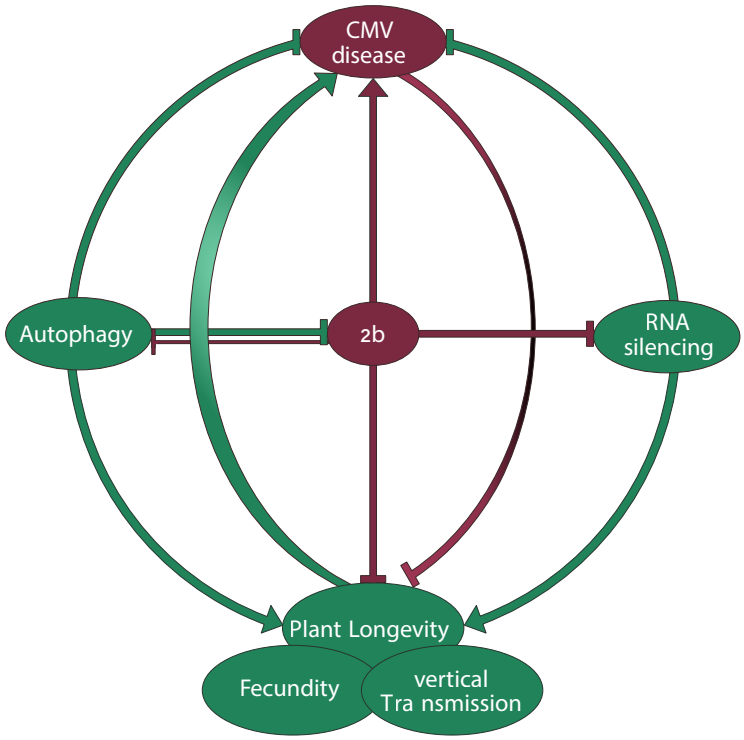

708

709 **Fig 7. Interplay between autophagy, RNA silencing and 2b shape CMV disease.**

710 The 2b protein is the major pathogenicity determinant in CMV infection. Plant autophagy
711 suppresses CMV accumulation through 2b degradation. By limiting 2b levels, autophagy
712 relaxes 2b mediated suppression of antiviral RNA silencing and virulence. Vice versa, 2b itself
713 has the capacity to restrict the plant autophagy response, but its significance during infection
714 remains to be resolved. Both autophagy and antiviral RNA silencing suppress virus
715 accumulation, and the lack of additivity between the pathways suggests their strong interaction
716 in the process, potentially through 2b. Taken together with their prominent synergism in disease
717 attenuation, we propose that autophagy and RNA silencing-based plant tolerance is not
718 quantitatively coupled to virus accumulation and that the pathways rather operate in a parallel
719 manner to promote survival of infected plants. Virulence evolution and trade-offs are
720 complicated for pathogens that utilize both vertical and horizontal transmission. Autophagy and
721 RNA silencing promotes CMV vertical transmission and likely also vector-mediated horizontal
722 transmission through increased plant longevity with only minor fitness penalties on virus

723 accumulation. We consider that CMV has adapted to and benefits from these potential antiviral
724 pathways. Thus, the interplay between the viral 2b protein, plant autophagy and RNA silencing
725 pathways determines the delicate balance between virus accumulation, transmission and plant
726 fitness in CMV disease.
727

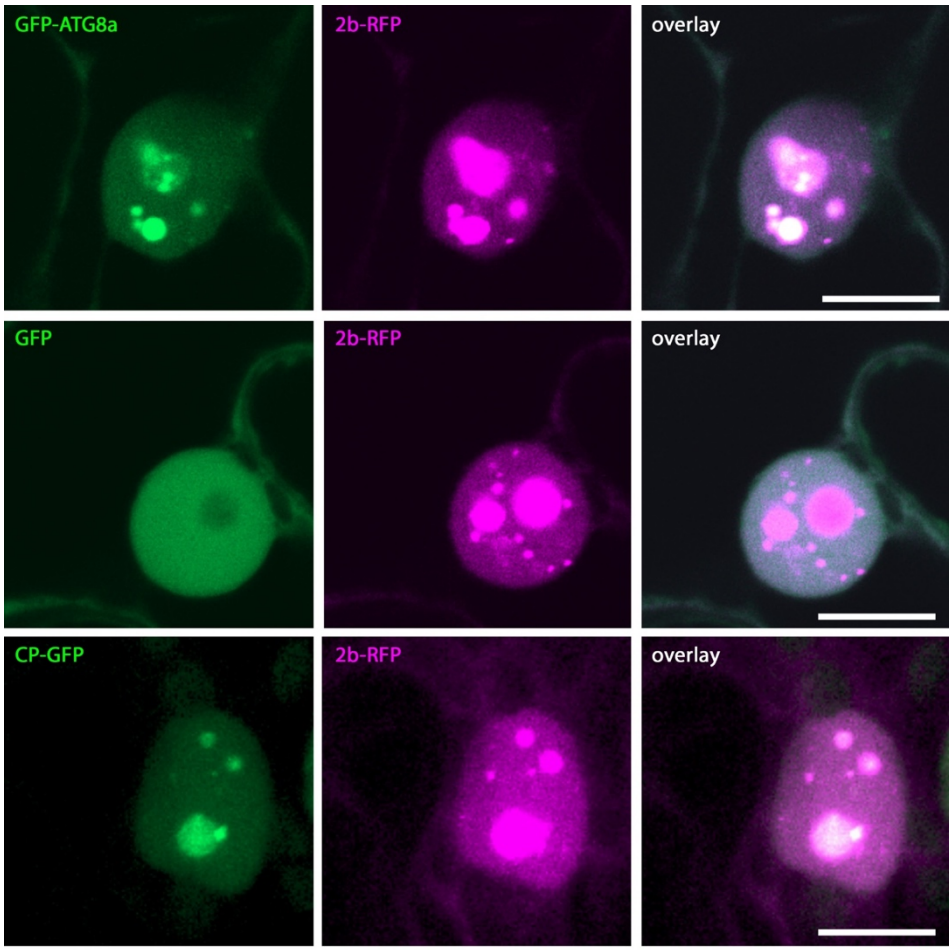

728

729

730 **S1 Fig. Nuclear localization analysis of 2b-RFP, GFP-ATG8a, GFP and CP-GFP.**

731 2b-RFP was co-expressed with GFP-ATG8a, GFP or CP-GFP in *N. benthamiana* and imaged

732 two days post agroinfiltration. GFP-ATG8a and GFP are single plains and CP-GFP a Z-stack

733 projection. Scale bar = 10 µm.

734

735

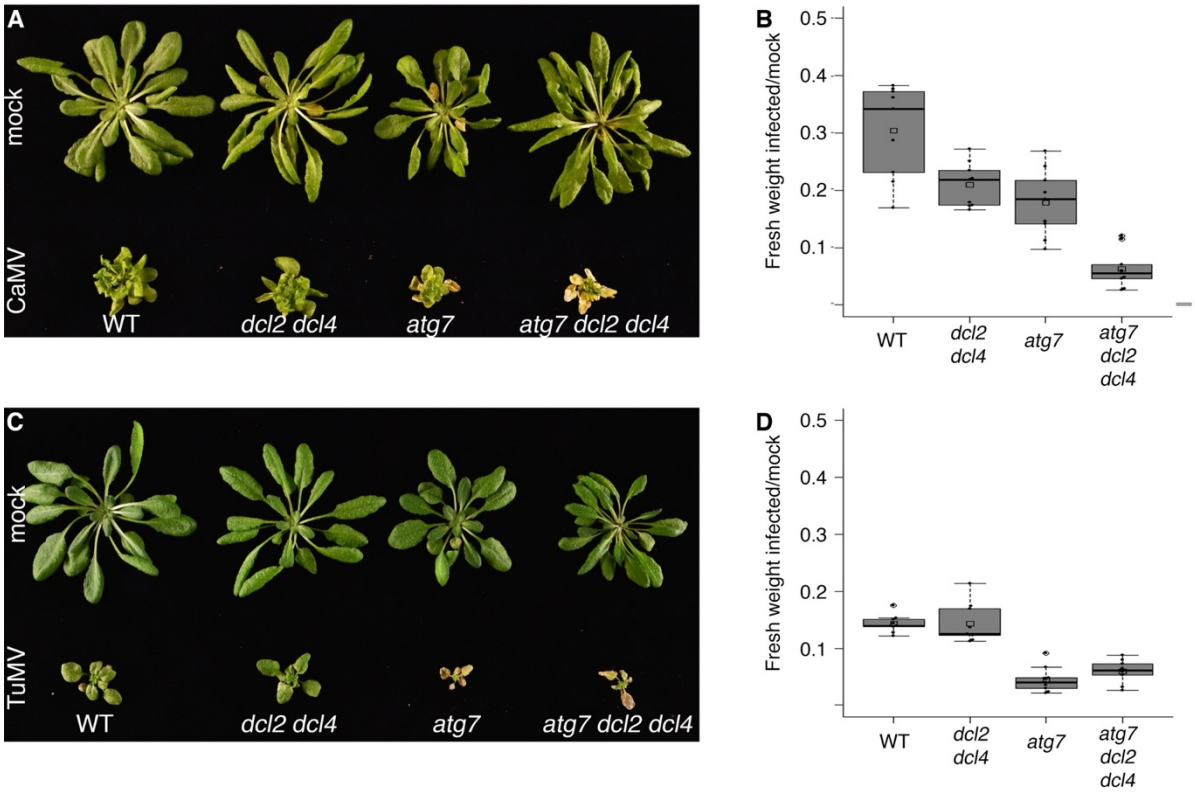

736

737

738 **S2 Fig. RNA silencing and autophagy provide additive protection against CaMV but not**

739 **TuMV disease.**

740 A) Representative image of mock and CaMV WT, *dcl2 dcl4*, *atg7* and *atg7 dcl2 dcl4* plants at

741 28 DAI. B) Fresh weight index representing the ratio between infected to mock plants. (*n*=9).

742 C) Representative image of mock and TuMV WT, *dcl2 dcl4*, *atg7* and *atg7 dcl2 dcl4* plants at

743 21 DAI. D) Fresh weight index representing the ratio between infected to mock plants. (*n*=9).

744

745

746

747

748

749